Proton Transport

DOI: 10.1002/ange.201102997

Confinement of Mobile Histamine in Coordination Nanochannels for Fast Proton Transfer**

*Daiki Umeyama, Satoshi Horike, Munehiro Inukai, Yuh Hijikata, and Susumu Kitagawa**

Proton-conducting solids, which act as the electrolyte of fuel cells, have received much attention. In particular, proton conductivity operating under anhydrous conditions and in the middle temperature region (>100 °C) is regarded as a significant target.[1] Heterogeneous hybridization of proton-conductive molecules (or polymers) and solid supports, such as amorphous silica and porous materials, is one of the approaches for the preparation of proton-conductive hybrids.[2]

Porous coordination polymers (PCPs) or metal–organic frameworks (MOFs), built by metal ions with bridging organic ligands, represent a new class of porous materials with high designability in composition, structure, and function.[3] To construct the proton conductors, we have focused on the hybridization of the proton carrier and PCP/MOFs on the molecular scale.[4] Several works on proton conductivity with PCP/MOF materials under high-humidity conditions have been reported, and the composites show a remarkable drop of conductivity when dehydrated.[5] Only two reports on PCP-based composites under anhydrous conditions have been published, including our previous work.[4,6] In both cases, incorporated proton carrier molecules transfer protons along the channels in ordered porous networks. However, the conductivities were not high enough to use the materials for practical systems. Therefore, other conductors having a conductivity above 10^{-3} S cm^{-1} under anhydrous conditions and in the middle temperature region are anticipated.[7]

In the work reported herein, we constructed the composite of aluminum-based microporous PCP and histamine, as the proton-donating molecule, and achieved a conductivity of over 10^{-3} S cm^{-1} at 150 °C in a completely anhydrous environment. $[Al(OH)(ndc)]_n$ (**1**, ndc = 1,4-naphthalenedicarboxylate), which has high thermo/chemo stabilities, was utilized as a support for the composite.[8] In previous work[4] we hybridized **1** with imidazole to give a conductivity of 10^{-5} S cm^{-1} at 120 °C. Compound **1** possesses one-dimensional channels with a 7.7×7.7 Å^2 pore diameter, as shown in Figure 1a. Histamine was introduced as a proton-donating/accepting molecule for hybridization. The melting point of histamine (83 °C) is lower than that of imidazole (89 °C), and three proton-donor/acceptor sites of an imidazole ring and an amine group act as the proton carrier (Figure 1b).

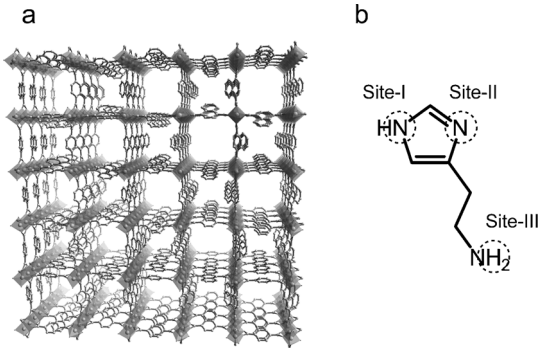

Figure 1. a) Crystal structure of $[Al(OH)(ndc)]_n$ (**1**). b) Schematic view of histamine with three proton-hopping sites.

The histamine does not undergo sublimation, which is different from imidazole, so we introduced the histamine into **1** by an immersion process. The activated powder of **1** was suspended with histamine and dry toluene and the suspension was heated to 95 °C, at which the histamine started to melt. After vacuum evacuation to remove toluene, we obtained a fine powder of composite **1** and histamine (**1⊃His**). The amount of histamine in **1⊃His** was checked by thermogravimetric analysis (TGA) measurement, which indicated that it contains 30 wt% of histamine. This corresponds to one histamine molecule per Al^{3+} ion, which is twice as large as that of the proton carrier in **1⊃Imidazole** (mol/mol).

Powder X-ray diffraction (XRD) of **1⊃His** suggested that the porous framework of **1** was maintained without any distortion. The solid-state cross polarization magic-angle spinning (MAS) ^{13}C NMR spectrum of **1⊃His** indicated the existence of histamine in the composite. Peaks corresponding to the carbon atoms of histamine in **1** were assigned by comparison with the spectrum of bulk histamine. CO_2 adsorption of **1⊃His** at 195 K (Figure 2a) was measured and the total uptake decreased compared with **1**, which suggested that histamine molecules occupied the micropore spaces of **1**.

[*] D. Umeyama, Dr. S. Horike, Dr. Y. Hijikata, Prof. Dr. S. Kitagawa
Department of Synthetic Chemistry and Biological Chemistry
Graduate School of Engineering, Kyoto University
Katsura, Nishikyo-ku, Kyoto 615-8510 (Japan)
E-mail: kitagawa@icems.kyoto-u.ac.jp
Prof. Dr. S. Kitagawa
Institute for Integrated Cell-Material Sciences (iCeMS)
Kyoto University, Yoshida, Sakyo-ku, Kyoto 606-8501 (Japan)
Prof. Dr. S. Kitagawa
Kitagawa Integrated Pore Project
Exploratory Research for Advanced Technology (ERATO)
Japan Science and Technology Agency (JST)
Kyoto Research Park Bldg #3, Shimogyo-ku, Kyoto 600-8815 (Japan)

[**] This work was supported by Grants-in-Aid for Scientific Research, Japan Society for the Promotion of Science (JSPS), The Murata Science Foundation, and ERATO Project, Japan Science and Technology Agency (JST).

Supporting information for this article is available on the WWW under http://dx.doi.org/10.1002/anie.201102997.

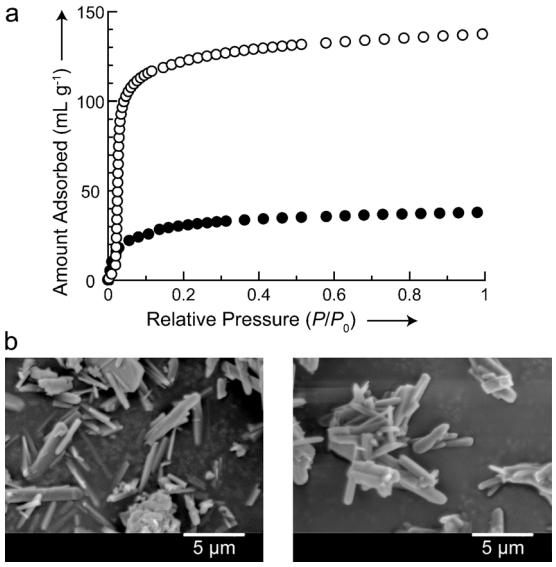

Figure 2. a) CO_2 adsorption isotherms of **1** (○) and **1⊃His** (●) at 195 K. b) SEM images of crystals of **1** (left) and **1⊃His** (right).

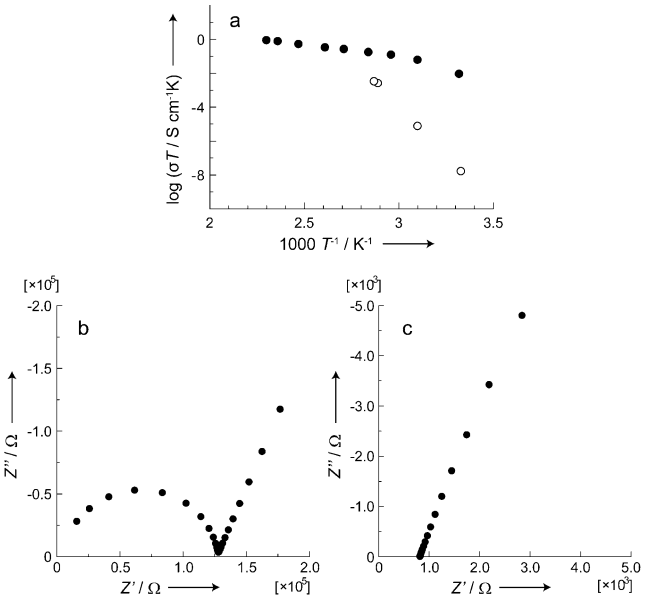

Figure 3. a) Arrhenius plots of conductivity of **1⊃His** (●) and bulk histamine (○) under anhydrous conditions. b, c) Nyquist plots of **1⊃His** at b) 25 and c) 110 °C.

We also obtained the SEM images of **1** and **1⊃His** (Figure 2b) and observed that the crystal morphology of **1⊃His** was similar to that of **1**, which indicated that the histamine molecules in the composite were accommodated inside the micropores of **1**, not aggregated on the outer surface. The TGA profile of **1⊃His** under a N_2 atmosphere showed no drop until 170 °C, which is desirable for conduction in a wide temperature range of over 100 °C. Note that if there were extra bulk histamine molecules on the outer crystal surface of **1**, we would observe the XRD pattern of bulk histamine and an exothermic peak by differential scanning calorimetry (DSC), but nothing was observed.

A sample for conductivity measurement was prepared by pelletizing powdered **1⊃His**. As reported previously, the proton conductivity of guest-free **1** is negligibly low.[4] Temperature-dependent conductivities were determined by using AC impedance spectroscopy. The measurement cell was filled with N_2 at atmospheric pressure. We observed a linear increase of conductivity as the temperature was elevated: 3.0×10^{-5} S cm^{-1} at room temperature to 1.7×10^{-3} S cm^{-1} at 150 °C (Figure 3a). The conductivity at room temperature was comparable to that of **1⊃Imidazole** at 120 °C.[4] Note that the conductivity of bulk histamine was 5.4×10^{-11} S cm^{-1} at room temperature and 9.4×10^{-6} S cm^{-1} at 75 °C, both of which were obviously lower than that of the composite. Bulk histamine starts to melt above 80 °C and we could not measure solid pellets at a higher temperature (Figure 3a).

Figure 3b and c show Nyquist plots of **1⊃His** at 25 and 110 °C, respectively. The former is a typical profile for temperatures below 50 °C and has one semicircle with a spur at low frequencies, which indicates blocking of protons at either the electrode or grain boundaries. The equivalent circuit $(R_bCPE_b)(CPE_{el})$ is adaptable for this case (where R_b is the resistance of proton transfer in the bulk phase and CPE_b and CPE_{el} are the constant-phase element in the bulk phase and electrode, respectively).[9] R_b is estimated by fitting experimental profiles. Figure 3c, on the other hand, is a typical profile for temperatures above 100 °C and a semicircle is not observed. This disappearance of the semicircle is accounted for by the decrease of the value of the time constant τ, which is the product of the values of resistance and capacitance. Because the capacitance values are almost constant (ca. 10^{-11} F), the decrease of τ is attributed to the decrease of R_b. This leads to a higher resonance frequency and the semicircle becomes out of range.[10] In this case, the value at the x-axis intercept is regarded as that of R_b, although the equivalent circuit is assumed to be the same. Gradual disappearance of the semicircle was observed from 60 to 100 °C. The conductivity at 150 °C is almost 100 times higher than that of **1⊃Imidazole** at 120 °C, and is comparable to those of the other polymer-based proton conductors recently studied under anhydrous conditions.[11]

We checked the content of histamine in **1⊃His** after washing it with organic solvent. Liquid ^{1}H NMR spectroscopy of **1⊃His** after degradation showed the same amount of histamine as that from TGA of the as-prepared sample, which supports the view that the amount of histamine attached to the outer crystal surface was negligible.

We investigated the mechanism of the high conductivity of **1⊃His** and the large difference in values for **1⊃His** and **1⊃Imidazole**. The conductivity depends on the concentration and mobility of the proton carrier. As mentioned above, the concentration of the carrier of **1⊃His** is twice as large as that of **1⊃Imidazole**, although the molecular volume of histamine (110 Å^3) is larger than that of imidazole (65 Å^3).[12] The histamine molecules in **1** were more densely packed than in the case of imidazole and formed an effective ion transporting path. When we introduced half the amount of histamine into **1**, **1⊃His** containing half the quantity of histamine was obtained. The conductivities were 6.4×10^{-7} S cm^{-1} at 25 °C

and $2.1\times10^{-4}\,S\,cm^{-1}$ at 150 °C, which were over ten times smaller than that of **1**⊃**His** with full loading. The conductivities are obviously larger than that of **1**⊃**Imidazole**, although the concentrations of histamine and imidazole are the same in **1**. These results suggest that the concentration of the proton carrier is critical for conductivity and also that there is an intrinsic difference between histamine and imidazole.

One distinct feature of **1**⊃**His** and **1**⊃**Imidazole** is the conformational structure of the proton carriers. The structure of histamine has been under intense study because of biological interest. It was revealed that various kinds of ionic states and conformations are possible depending on the chemical environment of the molecule, whereas crystalline histamine has only one conformation (the *trans* form).[13] Because the conductivity and activation energy are quite different from those of bulk histamine, histamine in the pore of **1** possibly has an appropriate conformation for proton hopping, where a shallow and uniform potential field is formed. Some of the conformations promote proton exchange by intramolecular hydrogen bonds between the amine group and imidazole ring. Because the rate-limiting step of proton hopping in the Grotthuss mechanism is molecular reorientation,[14] the intramolecular proton exchange in histamine leads to smooth reorientation of the molecules, which is not feasible for imidazole.

As mentioned above, bulk histamine exists in only the *trans* form with an intermolecular hydrogen bond between the N atom of the amino group and the H atom in the imidazole ring,[15] whereas the histamine in **1** could not form a bulklike crystal structure because of restricted space. The DSC profile of bulk histamine showed a sharp exothermic peak at the melting temperature (83 °C) and the **1**⊃**His** did not present a clear peak from room temperature to 100 °C, which suggested that the accommodated histamine did not undergo phase transition. Because we introduced melted histamine into **1**, it can be considered that the accommodated histamine molecules have a different packing system from bulk histamine.

To selectively observe the environment of histamine in **1** by solid-state ^{1}H NMR spectroscopy, we prepared **1d**⊃**His** (**1d**: [Al([D_6]ndc)(OH)]) in which all the protons except for the OH group in the framework of **1** were replaced by deuterium. The solid-state ^{1}H NMR spectra of bulk histamine at 298 and 318 K and of **1d** and **1d**⊃**His** at 298 K are shown in Figure 4. The single peak of **1d** at $\delta = 3$ ppm in Figure 4c is assigned to the OH group and the spectrum of bulk histamine at 298 K has broad peaks. The solid bulk histamine has crystallographically two independent positions in the structure, and the broadening of the spectrum is attributed mainly to a dipole–dipole interaction and large molecular anisotropy because of intermolecular hydrogen bonds.

Meanwhile, the spectrum of bulk histamine at 318 K (see Figure 4b) has more distinguishable peaks and we can assign each proton. Thermal activation of histamine promotes molecular isotropy showing the peak splitting. On the other hand, the spectrum of **1d**⊃**His** in Figure 4d has a similar shape to that in Figure 4b but each peak seems significantly sharper. This indicates that the accommodated histamine in **1d** at 298 K has isotropic behavior similar to the thermally activated bulk histamine and it contributes to effective proton

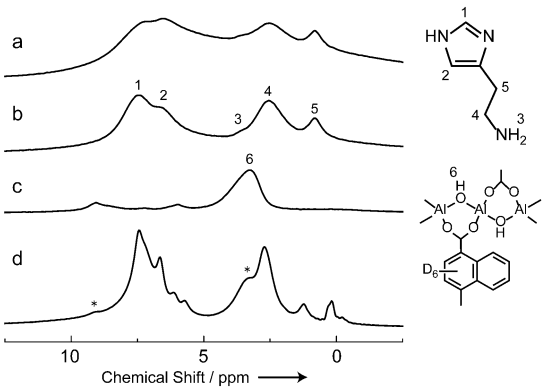

Figure 4. Solid-state MAS ^{1}H NMR spectra of bulk histamine at a) 298 and b) 318 K, and of c) **1d** and d) **1d**⊃**His** at 298 K. Asterisks are assigned to protons in the **1d** framework. Spinning rates are 15 kHz.

hopping. In fact, the activation energy of proton hopping of **1**⊃**His** was 0.25 eV, calculated by the Arrhenius equation. Such a low energy was also observed in other proton-conductive materials,[16] and this value is clearly smaller than for bulk histamine (2.3 eV) and reported anhydrous PCP/MOF conductors.[4,6] The high activation energy of bulk histamine results from its strong 3D intermolecular hydrogen bonds with a *trans* conformation. On the other hand, the dense packing and rich conformation of histamine in **1**, neither of which was observed in the case of imidazole, provided an effective environment for proton hopping. Solid-state MAS ^{27}Al NMR spectra of **1** and **1**⊃**His** were also measured and the obtained spectra were almost identical, thus indicating that the coordination environment around the Al^{3+} is unchanged even after histamine accommodation.

In conclusion, we have fabricated a proton-conductive composite that consists of histamine and aluminum PCP/MOF hybridized on the molecular scale. The hybridization method was simple and resulted in a conductivity of over $10^{-3}\,S\,cm^{-1}$ at 150 °C under anhydrous conditions. A rich structural conformation, molecular isotropy, and high concentration of histamine in **1** contribute to the remarkable improvement of conductivity. With its low activation energy, the material is regarded as a superionic conductor and the PCP supports are promising for the creation of hybrid conducting materials. Modification of the porous structure or morphology controls of the composite, such as alignment on substrates, are the next challenges.[17]

Received: May 1, 2011
Revised: July 25, 2011
Published online: October 11, 2011

Keywords: conducting materials · metal–organic frameworks · microporous materials · NMR spectroscopy · proton transport

[1] a) *Proton Conductors: Solids, Membranes and Gels—Materials and Devices* (Ed.: P. Colomban), Cambridge University Press, Cambridge, **1992**; b) H. G. Herz, K. D. Kreuer, J. Maier, G. Scharfenberger, M. F. H. Schuster, W. H. Meyer, *Electrochim. Acta* **2003**, *48*, 2165–2171; c) Q. F. Li, R. H. He, J. O. Jensen,

N. J. Bjerrum, *Chem. Mater.* **2003**, *15*, 4896 – 4915; d) C. Laberty-Robert, K. Valle, F. Pereira, C. Sanchez, *Chem. Soc. Rev.* **2011**, *40*, 961 – 1005.
[2] a) Z. W. Chen, B. Holmberg, W. Z. Li, X. Wang, W. Q. Deng, R. Munoz, Y. S. Yan, *Chem. Mater.* **2006**, *18*, 5669 – 5675; b) X. Li, E. P. L. Roberts, S. M. Holmes, V. Zholobenko, *Solid State Ionics* **2007**, *178*, 1248 – 1255; c) R. Marschall, I. Bannat, A. Feldhoff, L. Z. Wang, G. Q. Lu, M. Wark, *Small* **2009**, *5*, 854 – 859; d) S. Sanghi, M. Tuominen, E. B. Coughlin, *Solid State Ionics* **2010**, *181*, 1183 – 1188.
[3] a) O. M. Yaghi, H. L. Li, C. Davis, D. Richardson, T. L. Groy, *Acc. Chem. Res.* **1998**, *31*, 474 – 484; b) S. Kitagawa, R. Kitaura, S. Noro, *Angew. Chem.* **2004**, *116*, 2388 – 2430; *Angew. Chem. Int. Ed.* **2004**, *43*, 2334 – 2375; c) G. Férey, *Chem. Soc. Rev.* **2008**, *37*, 191 – 214; d) G. K. H. Shimizu, R. Vaidhyanathan, J. M. Taylor, *Chem. Soc. Rev.* **2009**, *38*, 1430 – 1449; e) L. J. Murray, M. Dincă, J. R. Long, *Chem. Soc. Rev.* **2009**, *38*, 1294 – 1314.
[4] S. Bureekaew, S. Horike, M. Higuchi, M. Mizuno, T. Kawamura, D. Tanaka, N. Yanai, S. Kitagawa, *Nat. Mater.* **2009**, *8*, 831 – 836.
[5] a) H. Kitagawa, Y. Nagao, M. Fujishima, R. Ikeda, S. Kanda, *Inorg. Chem. Commun.* **2003**, *6*, 346 – 348; b) T. Yamada, M. Sadakiyo, H. Kitagawa, *J. Am. Chem. Soc.* **2009**, *131*, 3144 – 3145; c) S. Ohkoshi, K. Nakagawa, K. Tomono, K. Imoto, Y. Tsunobuchi, H. Tokoro, *J. Am. Chem. Soc.* **2010**, *132*, 6620 – 6621.
[6] J. A. Hurd, R. Vaidhyanathan, V. Thangadurai, C. I. Ratcliffe, I. L. Moudrakovski, G. K. H. Shimizu, *Nat. Chem.* **2009**, *1*, 705 – 710.
[7] a) M. Yamada, I. Honma, *Polymer* **2004**, *45*, 8349 – 8354; b) S. U. Çelik, U. Akbey, R. Graf, A. Bozkurt, H. W. Spiess, *Phys. Chem. Chem. Phys.* **2008**, *10*, 6058 – 6066; c) V. Di Noto, E. Negro, J. Y. Sanchez, C. Iojoiu, *J. Am. Chem. Soc.* **2010**, *132*, 2183 – 2195.
[8] A. Comotti, S. Bracco, P. Sozzani, S. Horike, R. Matsuda, J. Chen, M. Takata, Y. Kubota, S. Kitagawa, *J. Am. Chem. Soc.* **2008**, *130*, 13664 – 13672.
[9] E. Barsoukov, J. R. Macdonald, *Impedance Spectroscopy*, Wiley Interscience, New York, **2005**.
[10] a) Y. Inaguma, Y. Matsui, Y. J. Shan, M. Itoh, T. Nakamura, *Solid State Ionics* **1995**, *79*, 91 – 97; b) X. Wang, P. Xiao, *J. Eur. Ceram. Soc.* **2002**, *22*, 471 – 478; c) W. L. Li, L. X. Xu, D. Luo, H. M. Wu, J. P. Tu, M. J. Yang, *Eur. Polym. J.* **2007**, *43*, 522 – 528.
[11] a) M. Schuster, W. H. Meyer, G. Wegner, H. G. Herz, M. Ise, M. Schuster, K. D. Kreuer, J. Maier, *Solid State Ionics* **2001**, *145*, 85 – 92; b) T. Tezuka, K. Tadanaga, A. Hayashi, M. Tatsumisago, *J. Am. Chem. Soc.* **2006**, *128*, 16470 – 16471; c) Y. Chen, M. Thorn, S. Christensen, C. Versek, A. Poe, R. C. Hayward, M. T. Tuominen, S. Thayumanavan, *Nat. Chem.* **2010**, *2*, 503 – 508.
[12] The volumes of the molecules were determined using MOPAC 7.
[13] a) J. A. Collado, I. Tunon, E. Silla, F. J. Ramirez, *J. Phys. Chem. A* **2000**, *104*, 2120 – 2131; b) M. Kraszni, J. Kokosi, B. Noszal, *J. Chem. Soc. Perkin Trans. 2* **2002**, 914 – 917; c) E. D. Raczyńska, M. Darowska, M. K. Cyranski, M. Makowski, T. Rudka, J. F. Gal, P. C. Maria, *J. Phys. Org. Chem.* **2003**, *16*, 783 – 796.
[14] M. Mizuno, S. Hayashi, *Solid State Ionics* **2004**, *167*, 317 – 323.
[15] J. J. Bonnet, J. A. Ibers, *J. Am. Chem. Soc.* **1973**, *95*, 4829 – 4833.
[16] a) Y. Nishiyama, K. Ochi, N. Nishiyama, Y. Egashira, K. Ueyama, Y. Egashira, K. Ueyama, *Electrochem. Solid-State Lett.* **2008**, *11*, B6 – B9; b) H. L. Tang, M. Pan, S. F. Lu, J. L. Lu, S. P. Jiang, *Chem. Commun.* **2010**, *46*, 4351 – 4353.
[17] a) T. Bein, E. Biemmi, C. Scherb, *J. Am. Chem. Soc.* **2007**, *129*, 8054 – 8055; b) W. Q. Jin, Y. X. Hu, X. L. Dong, J. P. Nan, X. M. Ren, N. P. Xu, Y. M. Lee, *Chem. Commun.* **2011**, *47*, 737 – 739; c) R. Makiura, S. Motoyama, Y. Umemura, H. Yamanaka, O. Sakata, H. Kitagawa, *Nat. Mater.* **2010**, *9*, 565 – 571.

